

The star formation timescale of elliptical galaxies

Fitting [Mg/Fe] and total metallicity simultaneously

Zhiqiang Yan^{1,2}, Tereza Jerabkova^{1,2,3,4,5}, and Pavel Kroupa^{1,2}.

¹ Helmholtz-Institut für Strahlen- und Kernphysik (HISKP), Universität Bonn, Nussallee 14–16, 53115 Bonn, Germany
Emails: yan@astro.uni-bonn.de; tereza.jerabkova@eso.org; pkroupa@uni-bonn.de

² Charles University in Prague, Faculty of Mathematics and Physics, Astronomical Institute, V Holešovičkách 2, CZ-180 00 Praha 8, Czech Republic

³ Astronomical Institute, Czech Academy of Sciences, Fričova 298, 25165, Ondřejov, Czech Republic

⁴ Instituto de Astrofísica de Canarias, E-38205 La Laguna, Tenerife, Spain

⁵ GRANTECAN, Cuesta de San Jose s/n, 38712 Brena Baja, La Palma, Spain

Received 5 Sep 2019 / Accepted 29 Oct 2019

ABSTRACT

The alpha element to iron peak element ratio, for example [Mg/Fe], is a commonly applied indicator of the galaxy star formation timescale (SFT) since the two groups of elements are mainly produced by different types of supernovae that explode over different timescales. However, it is insufficient to consider only [Mg/Fe] when estimating the SFT. The [Mg/Fe] yield of a stellar population depends on its metallicity. Therefore, it is possible for galaxies with different SFTs and at the same time different total metallicity to have the same [Mg/Fe]. This effect has not been properly taken into consideration in previous studies. In this study, we assume the galaxy-wide stellar initial mass function (gwIMF) to be canonical and invariant. We demonstrate that our computation code reproduces the SFT estimations of previous studies where only the [Mg/Fe] observational constraint is applied. We then demonstrate that once both metallicity and [Mg/Fe] observations are considered, a more severe "downsizing relation" is required. This means that either low-mass ellipticals have longer SFTs (> 4 Gyr for galaxies with mass below $10^{10} M_{\odot}$) or massive ellipticals have shorter SFTs (≈ 200 Myr for galaxies more massive than $10^{11} M_{\odot}$) than previously thought. This modification increases the difficulty in reconciling such SFTs with other observational constraints. We show that applying different stellar yield modifications does not relieve this formation timescale problem. The quite unrealistically short SFT required by [Mg/Fe] and total metallicity would be prolonged if a variable stellar gwIMF were assumed. Since a systematically varying gwIMF has been suggested by various observations this could present a natural solution to this problem.

1. Introduction

The stellar α element to iron peak element ratio, for example [Mg/Fe], is a classic indicator of the star formation timescale (SFT) for galaxies (applied in, e.g. Thomas et al. 2005, Segers et al. 2016, Liu et al. 2016b, Kriek et al. 2019, and Dabringhausen 2019). It is known that possibly more than half of the iron in the Universe is produced by Type Ia supernovae (SNIa) which explode on average about a billion years after the formation of their parental stellar population (e.g., Maoz & Mannucci 2012). On the other hand, α elements are mainly produced by type II supernovae (SNII) which happen within tens of millions of years when the most massive stars come to the end of their lifetime. Consequently, $[\alpha/\text{Fe}]$ of the gas polluted by the supernovae decreases over time starting from the highest value, that is the $[\alpha/\text{Fe}]$ yield of the most massive star. When new stars are born from the cooled and recycled polluted gas, the formation time of a star is marked by its $[\alpha/\text{Fe}]$. Thus the longer the SFT of a galaxy, the lower its average stellar $[\alpha/\text{Fe}]$. With the help of galaxy chemical-evolution simulations, Thomas et al. (2005) were able to derive an approximated relation between average stellar $[\alpha/\text{Fe}]$ and the SFT of a galaxy, t_{sf} :

$$[\alpha/\text{Fe}] \approx 1/5 - 1/6 \cdot \log(t_{\text{sf}}). \quad (1)$$

This relation indicates that the averaged stellar $[\alpha/\text{Fe}]$ of a galaxy (when the galaxy is 12 Gyr old) is a function of its SFT. More comprehensive consideration shows that the resulting $[\alpha/\text{Fe}]$ should also depend on the metallicity of the galaxy (see below).

Since there is compelling evidence that more massive elliptical galaxies typically have a higher stellar $[\alpha/\text{Fe}]$, it has been generally accepted that massive ellipticals should have shorter SFTs (Pipino & Matteucci 2004; Pipino et al. 2009; Thomas et al. 2005, 2010). This is known as downsizing of the SFT¹, which contradicts the cosmological merger tree in the standard Λ CDM universe (Fontanot et al. 2009). We note that throughout this text, 'downsizing' refers to the SFT.

It seems that downsizing can be realized quite readily when assuming elliptical galaxies form in a monolithic collapse with in situ star formation dominating the stellar mass of the ellipticals and by tuning the baryonic feedback processes due to SNII and/or active galactic nucleus (Pipino & Matteucci 2004, 2006). However, this only ensures that galaxies stop star formation within the required timescale but does not ensure that galaxies can grow enough stellar mass in such a short time when hydrodynamic constraints are applied. This means that the assumed gas infall rate and/or star formation efficiency used as free parameters in the model of Pipino & Matteucci (2004) might be unrealistically high. Indeed, Matteucci (1994, their section 5) pointed out that the dynamical free-fall time increases for more massive gas clouds and may require a merging process with

¹ Not to be confused with the downsizing of the galaxy age or star formation rate (SFR), which is the original meaning of downsizing (Cowie et al. 1996). See Fontanot et al. (2009) for a summary of the many manifestations of downsizing.

higher collision velocities to achieve the mass growth of more massive ellipticals in a shorter timescale. The galactic mass–metallicity correlation also requires that such merging processes happen early, before most stars form. Otherwise, the more massive galaxy would have the same stellar chemical composition as its lower-mass component galaxies. We note that the star formation of elliptical galaxies also needs to be early, before the gas fully exchanges angular momentum and becomes a disk. Cosmological simulations struggle in fulfilling all these requirements. Under the standard hierarchical model of galaxy formation, mergers usually occur between galaxies that have already formed a stellar population. When dry mergers (without significant amounts of gas) are an important channel for the mass growth of elliptical galaxies, that is when stellar mass grows mostly from ex situ contributions, baryonic feedback during the merger does not affect the pre-existing stellar populations. Thus, the feedback is not efficient enough to cause the required level of downsizing, and the observed [Mg/Fe]–galaxy-mass relation cannot be reproduced in Nagashima et al. (2005) and Gargiulo et al. (2015) when an invariant galaxy-wide stellar initial mass function (gwIMF) is assumed. But see also Pipino et al. (2009) mimicking the monolithic formation behaviour and Calura & Menci (2011) enhancing in situ star formation triggered by fly-by encounter events.

In addition to the above difficulties, there is a more imperative problem. The observed more massive ellipticals have both a higher [Mg/Fe] value and higher metallicity (Thomas et al. 2010; Johansson et al. 2012; Conroy et al. 2014). However, the galaxy models which reproduce the $[\alpha/\text{Fe}]$ –galaxy-mass relation do not simultaneously reproduce the metallicity–galaxy-mass relation. This problem has been recognised since 2009 by Pipino et al. (2009) and Calura & Menci (2009) and recently confirmed by Fontanot et al. (2017) and De Masi et al. (2018) where a variable gwIMF is suggested to be necessary once [Mg/Fe] and metallicity observations are considered together. The cause of this is stated clearly both in De Lucia et al. (2017), applying a semi-analytic model, GAEA, and Okamoto et al. (2017), applying cosmological hydrodynamical simulations, that is, the SFT required to reproduce the high $[\alpha/\text{Fe}]$ value being too short, such that there is not enough time for gas to recycle and enrich, resulting in a reversed metallicity–galaxy-mass relation for massive galaxies. More recent studies have not solve this problem. For example, Barber et al. (2018), following Segers et al. (2016), show that the hydrodynamical simulation EAGLE can reproduce the [Mg/Fe]–mass relation but not the metallicity–galaxy-mass relation, and variable IMFs are suggested; while Pantoni et al. (2019) do not reproduce the trend of the [Mg/Fe]–galaxy-mass relation (cf. Liu et al. 2016a). In summary, it is strongly suggested that an invariant gwIMF is not able to reproduce both the $[\alpha/\text{Fe}]$ –galaxy-mass and metallicity–galaxy-mass relations, but a conclusive study is lacking.

With this contribution, we demonstrate that even without hydrodynamical considerations, that is without the complication of a non-zero gas recycling time, it is not possible to reproduce [Mg/Fe] and total metallicity simultaneously with realistic SFTs, thus strongly challenging the downsizing scheme. We point out that the estimation of SFT should depend not only on $[\alpha/\text{Fe}]$, as is the case for Eq. 1, but also on total metallicity of the stars. Massive stars with higher initial metallicity have a lower [Mg/Fe] yield because the stronger stellar wind of these stars mainly reduces the α element production (Matteucci 2012, section 2.1.3 there). This is shown in Yan et al. (2019, their figure 4) who applied the stellar yield of massive stars from Portinari et al. (1998, see their figure 7 to 9). The Nomoto et al. (2013)

stellar yield also agrees with this trend. We note that the aforementioned studies only provide stellar yields with stellar initial metallicities $[Z]=\log_{10}(Z/Z_{\odot})>-2$, where Z_{\odot} is the solar metallicity. The Chieffi & Limongi (2004) stellar yield table extends to $[Z]=-4$ and $Z=0$, suggesting a reversed trend when $[Z]<-2$. However, even if such behaviour is real, it only affects the very first generation of stars and has (if at all) a negligible effect on the galaxy chemical evolution. Thus, once the metallicity of the stellar population is considered, the estimation of the SFT is different and it becomes impossible to explain the observed variation of [Mg/Fe] solely by adjusting the SFT.

This paper is organised as follows. First we introduce the observations and the procedure used to estimate the SFT in Sections 2 and 3, respectively. Our result, fitting only the [Mg/Fe] observation, reproduces the downsizing relation suggested by previous studies (this validates our chemical evolution code), while the result from fitting both [Mg/Fe] and total metallicity suggests a more severe downsizing relation, as is shown in Section 4. Possible variations on the adopted stellar yield table, star formation history (SFH), and the gwIMF are discussed in Section 5. We conclude that even with a modified stellar yield the required SFT is either too short for the massive galaxies or too long for the low-mass galaxies, compared to independent SFT constraints summarized in Section 6. Finally, we conclude in Section 7 that a systematic variation of the gwIMF appears to be a promising solution. In line with previous studies (Vazdekis et al. 1996, 1997; Recchi et al. 2009; Calura & Menci 2009; Weidner et al. 2013; Fontanot 2014; Recchi & Kroupa 2015; Vincenzo et al. 2015; Gargiulo et al. 2015; Fontanot et al. 2017; De Masi et al. 2018).

A comprehensive discussion of the likelihood of variable IMF formulations given the metallicity/[Mg/Fe]–galaxy-mass relation (considering possible systematic observational errors in galaxy element abundances, see Section 2) is performed in our accompanying paper (Yan et al. 2020, in prep.).

2. Data

2.1. $[Z/X]$ –galaxy-mass relation

We adopt the typical metallicity–galaxy-mass relation of E- and S0-type galaxies from Arrigoni et al. (2010, their table B1). The notation of metallicity is changed from $[Z/H]$ to $[Z/X]$ following Yan et al. (2019, their equation 6). We note that the $[Z/X]$ –galaxy-mass relation depends on the galaxy type. A lower mean metallicity is suggested when considering all types of galaxies (Gallazzi et al. 2005). The data of single galaxies are shown by the crosses in Fig. 1. They illustrate that the scatter of $[Z/X]$ values for a given galaxy-mass is larger for lower-mass galaxies. To estimate the mean and standard deviation of the $[Z/X]$ –galaxy-mass relation, we randomly generate 1000 realizations for each data point assuming that the observational error has a normal distribution on the $[Z/X]$ value. When the given error is asymmetric, we assume the probability distribution above and below the data value is half a normal distribution. We then calculate the mean and the standard deviation of the metallicity with a given galaxy mass using all the realized galaxies that have a mass within ± 0.5 dex of the given galaxy mass, where the 0.5 dex is approximately the typical mass uncertainty for a single galaxy. The results are shown by the solid and dashed lines in Fig. 1.

2.2. [Mg/Fe]–galaxy-mass relation

The procedure of calculating the mean and standard deviation of [Mg/Fe] values of galaxies with different masses is simpler as it can be well described by a linear relation with a negligible fitting error. See for example the data in Arrigoni et al. (2010) and an assembly of data in Liu et al. (2016a) where the [Mg/Fe] values have a typical observational error of 0.05 dex for a given galaxy and a standard deviation of less than 0.1 dex for galaxies with a given mass (when the galaxy mass is larger than about $10^{9.5} M_{\odot}$). In order to compare our results with the previous SFT study, we adopt the [Mg/Fe]–galaxy-mass relation of Thomas et al. (2005, their equation 3) as the mean and assume a standard deviation of 0.1 dex as is shown by the dashed lines in Fig. 2. Thus the [Mg/Fe] data of single galaxies are neither used nor plotted. We note that this assumption is only made to reproduce the work done by Thomas et al. (2005) as detailed in Section 4.1 below. Adopting a different [Mg/Fe]–galaxy-mass relation, for example shifting the relation vertically, would not affect our main conclusions (cf. Section 5.1.1).

We note that there is a systematic observational uncertainty due to the different assumptions applied in the stellar synthesis model (stellar evolution and atmosphere model). This is shown for example by the mismatch of the intercept of the fit between five different studies compared in Conroy et al. (2014, their figure 18), which can be as large as 0.1 dex. This indicates that the slope, rather than the intercept, of the galaxy-mass–[Mg/Fe] relation contains the most reliable information. Fortunately, it is also the case that the intercept of this relation is uncertain in galaxy evolution models due to the larger uncertainty of stellar yields, while the slope is largely unaffected under different yield assumptions (see Section 5.1). Thus, it is possible to unearth some truth about the galaxies even when the observational metal abundance and the stellar yields are both unsettled.

2.3. Dynamical mass

To compare the chemical composition of the observed galaxies and our galaxy models for a given galaxy mass, we first need to clarify the definition of the galaxy mass where the data is adopted from, that is Arrigoni et al. 2010 and Thomas et al. 2005, which we discuss separately in the following paragraphs.

Arrigoni et al. 2010, from whom we adopted the metallicity–galaxy-mass relation, estimated the mass of a galaxy within the effective radius from the velocity dispersion in the galactic centre and effective radius using the virial theorem (see also Burstein et al. 1997 and Trager et al. 2000). This is defined as the dynamical mass of a galaxy, M_{dyn} , which is independent of gwIMF as pointed out by Thomas et al. (2010, their section 3.7). The estimation of M_{dyn} in Arrigoni et al. (2010, their equation B1) using central velocity dispersion assumes the luminosity profile of the ellipticals (cf. Binney & Tremaine 2008, their equation 4.249b) in which dark matter and gas contribute a mass portion within the effective radius from (i) negligible (e.g. Binney & Tremaine 2008, their section 4.9.2 and Buote & Barth 2019, their figure 6) to (ii) a few tens of percent (e.g. Thomas et al. (2011)). In case (i), assuming that the stellar remnant mass profile follows the stellar mass profile, and both follow the luminosity profile, the observational M_{dyn} is approximately the mass of living stars and stellar remnants within the effective radius. Thus, the M_{dyn} in Arrigoni et al. (2010) is comparable with the M_{mod} of our model, which is the total mass of living stars and stellar remnants of a modelled galaxy at 14 Gyr. On the other hand, in case (ii), M_{dyn} is larger than M_{mod} and they cannot be compared di-

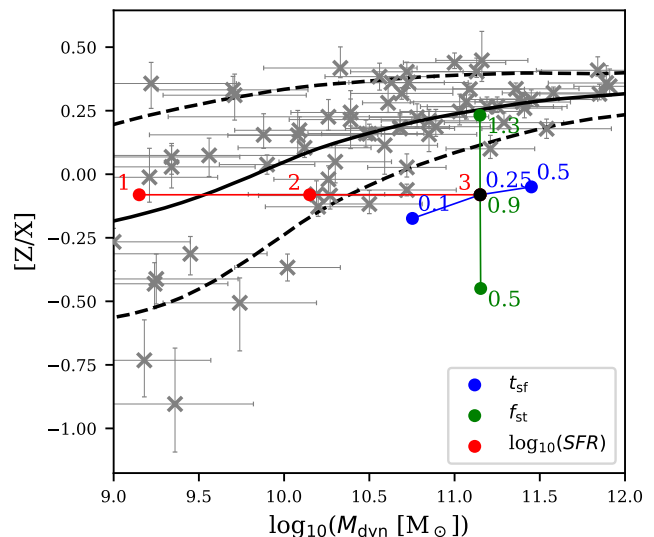


Fig. 1. Observed relation between galaxy mass and metallicity, $[Z/X]$ for local E- and S0-type galaxies. The $[Z/X]$ data adopted from Arrigoni et al. (2010) are shown as crosses. The mean and standard deviation derived from the data are given as the solid and the dotted lines (see Section 2). Modeled stellar-mass-weighted $[Z/X]$ of galaxies at 14 Gyr with a given SFT, t_{sf} (0.1, 0.25, or 0.5 Gyr), accumulated star formation fraction, f_{st} (0.5, 0.9, or 1.3), and SFR, SFR (10, 100, or 1000 M_{\odot}/yr), assuming the invariant canonical gwIMF, are plotted with coloured filled circles. The results are shown when varying only one of the above parameters in comparison with the black filled circles.

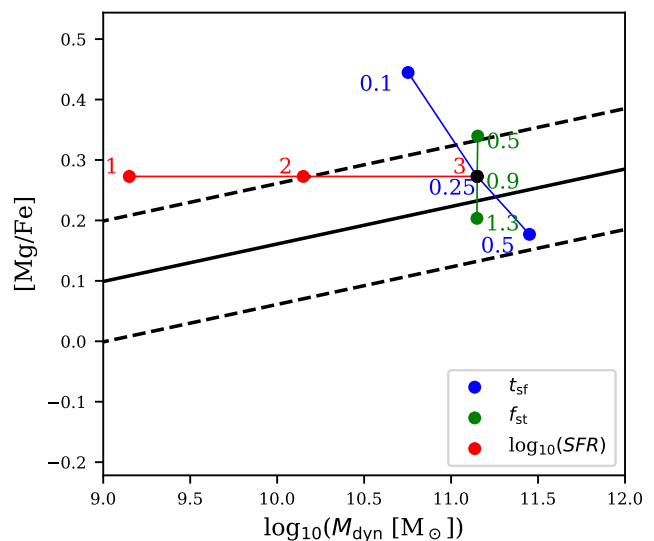


Fig. 2. The [Mg/Fe]–galaxy-mass relation given in Thomas et al. (2005) (solid line) and the assumed 0.1 dex standard deviation region (the dashed lines, see Section 2). Coloured filled circles are the same as in Fig. 1 but for [Mg/Fe] values.

rectly. Therefore, we also checked that defining M_{mod} to be ten times larger than the current definition (i.e. ten times the mass of living stars and stellar remnants), that is to shift our calculation results (filled circles in Fig. 1 and 2) horizontally by 1 dex, would lead to insignificant changes in our results in the following sections. If we were to set M_{mod} to be one hundred times the

mass of living stars and stellar remnants in the model, the results in the following sections would be different but the general trend would be preserved and so would the conclusions that follow. Thus, the discussion below is robust under different dark matter and gas mass portions.

It is possible to further simplify the mass estimation (with the help of certain gwIMF assumptions) by applying the empirical Kormendy relation (Kormendy 1977; e.g. Recchi et al. 2009) or, equivalently, using the Faber-Jackson relation (Faber & Jackson 1976; e.g. Thomas et al. 2005, their equation 2) such that the galaxy mass is solely a function of central velocity dispersion. From Thomas et al. (2005, their equation 3) we adopt the [Mg/Fe]–galaxy-mass relation. The "stellar mass", $M_{*,\text{tot}}$, in this given relation actually includes stellar remnants, as they are part of the mass-to-light ratio calculated for a stellar population, hence $M_{*,\text{tot}}$ is equal to our M_{mod} and we can safely apply Thomas et al. (2005, their equation 3) and replace the $M_{*,\text{tot}}$ symbol with M_{dyn} .

3. Method

3.1. Calculation of galaxy chemical evolution

In our fiducial model, we assume the monolithic collapse formation scenario of elliptical galaxies and a gwIMF which has the same shape as the canonical invariant IMF given in Kroupa (2001, their equation 2). The simulation is performed with the open-source galaxy chemical evolution model developed by Yan et al. (2019) which allows pre-specification of the SFH (cf. Thomas et al. 1999). This scheme adopts the stellar yield tables from, Marigo (2001) and Portinari et al. (1998) for AGB and massive stars, respectively, SNIa yields from Gibson et al. (1997, their TNH93 dataset), the delay time distribution of SNIa given by Maoz & Mannucci (2012), no gas flows, and instantaneous-well-mixing of the gas, that is we treat the galaxy as an isolated point.

For each galaxy model, we specify a different initial gas mass and a SFH defined by some constant SFR, SFR , over a given SFT, t_{sf} , that is, a box-shaped SFH. The initial gas mass is determined by multiplying the summed initial mass of all the stars ever formed (according to the assumed SFH) and an accumulated star formation fraction parameter, f_{st} . That is, the f_{st} parameter is defined as the ratio between the accumulated stellar initial mass and the initial gas mass of the simulation. All applied parameters are listed in Table 1 which has in total $6 \times 7 \times 15 = 630$ possible configurations.

We note that the parameter f_{st} is different to the parameter f_{trans} defined in Thomas et al. (1999). The parameter f_{trans} is not an accumulated value and cannot be larger than one. However, the largest possible f_{st} value is 1.5 if all the stellar populations return one-third of their masses instantaneously after their formation due to deceased stars, which is approximately the case when assuming the canonical gwIMF and instantaneous recycling.

The outputs of each computation are the properties of the galaxy when it is 14 Gyr old. We note that the stellar-mass-weighted property of the galaxy does not vary significantly after a few billion years as we assume a box-shaped SFH and there is no star formation activity at later times (Yan et al. 2019). The results include galactic dynamical mass (mass of living star plus stellar remnant mass), M_{dyn} , mass-weighted stellar metallicity, $[Z/X]$, and mass-weighted stellar [Mg/Fe]. We define

$$[Z/X] = \log_{10}(Z/X) - \log_{10}(Z_{\odot}/X_{\odot}), \quad (2)$$

where $Z_{\odot} = 0.01886$ and $X_{\odot} = 0.70683$ are the solar mass fraction of metal and hydrogen adopted from Anders & Grevesse (1989).

An example of the output is shown in Figs. 1 and 2 (filled circles), which demonstrates the variation of the resulting $[Z/X]$ and [Mg/Fe] values due to modifications of the initial parameters. The black filled circles are resulting from a galaxy computation with input parameters being $t_{\text{sf}} = 0.25$ Gyr, $f_{\text{st}} = 0.9$, and $SFR = 1000 M_{\odot}/\text{yr}$. Coloured filled circles show how the results change when varying one of the three parameters. It turns out that varying the SFR has no effect on the chemical evolution in our fiducial model; a longer SFT reduces [Mg/Fe] as expected and mildly increases $[Z/X]$ due to an increased number of recycling epochs (i.e. a larger number of formed stellar populations); the f_{st} parameter influences $[Z/X]$ significantly and also decreases [Mg/Fe] for a higher $[Z/X]$. This originates from the fact that massive metal-rich stars have a lower [Mg/Fe] yield, as is mentioned above in Section 1.

3.2. Calculating the likelihood of each parameter set

The output values of $[Z/X]$ and [Mg/Fe] for all models with different sets of parameters are then fitted with the observations thus determining the likelihood for each parameter configuration in Table 1. In order to make the result smoother, we linearly interpolated the model grid calculation results of $[Z/X]$ and [Mg/Fe] for any t_{sf} , f_{st} , and M_{dyn} combination.

The likelihood of a given parameter set, $p(M_{\text{dyn}}, f_{\text{st}}, t_{\text{sf}})$, is calculated using the interpolated results, $[Z/X]_{\text{mod}}$ and $[\text{Mg}/\text{Fe}]_{\text{mod}}$, as:

$$\begin{aligned} p(M_{\text{dyn}}, f_{\text{st}}, t_{\text{sf}}) &= p_{Z/X} \times p_{\text{Mg/Fe}}, \\ p_{Z/X} &= \\ &1 - \text{erf} \left[\left([Z/X]_{\text{obs}} - [Z/X]_{\text{mod}}(M_{\text{dyn}}, f_{\text{st}}, t_{\text{sf}}) \right) / \sigma_{Z/X} / \sqrt{2} \right], \\ p_{\text{Mg/Fe}} &= \\ &1 - \text{erf} \left[\left([\text{Mg}/\text{Fe}]_{\text{obs}} - [\text{Mg}/\text{Fe}]_{\text{mod}}(M_{\text{dyn}}, f_{\text{st}}, t_{\text{sf}}) \right) / \sigma_{\text{Mg/Fe}} / \sqrt{2} \right], \end{aligned} \quad (3)$$

where the erf stands for the error function, σ is the standard deviation of the observation, and the subscript obs and mod stand for the observational value and the value interpolated from our model grid, respectively.

4. Results

With a given f_{st} , we are able to condense the $p(M_{\text{dyn}}, f_{\text{st}}, t_{\text{sf}})$ information into the $t_{\text{sf}}-M_{\text{dyn}}$ plane with the likelihood p of each point presented by a colour code. The f_{st} is either set to be a fixed value (as in Section 4.1 and 4.2.1 below) or is a free parameter such that only the best-fit results are shown (as in Section 4.2.2).

4.1. Reproducing previously achieved results

Thomas et al. (2005) discussed the SFT based on the α element enhancement of early-type galaxies (Eq.1). As mentioned above, this earlier study considers only the [Mg/Fe] values. The assumption on the mass ratio between star and gas (i.e. f_{st}) of Thomas et al. (2005) is unclear according to their section 6.1. To test if our code can reproduce this previous result, we can only assume that Thomas et al. (2005) applied an invariant f_{st} . This is reasonable because Thomas et al. (1999) discussed and demonstrated mainly the [Fe/H] and [Mg/Fe] evolution and not

Table 1. Free parameters in the model

Parameter [Unit]	Meaning	Applied values
$\log_{10}(SFR[M_{\odot}/\text{yr}])$	galaxy-wide star formation rate	-1, 0, 1, 2, 3, 4, (5), (6) ^b
t_{sf} [Gyr]	galactic star formation timescale	0.05, 0.1, 0.25, 0.5, 1, 2, 4
f_{st}	accumulated star formation fraction ^a	0.1, 0.2, 0.3, ..., 1.5

Notes. ^(a) The ratio between the accumulated stellar initial mass of all the stars ever formed (according to the assumed SFH) and the initial gas mass of the simulation. This value can be larger than one since the stars return their mass into the gas phase when they die. The returned gas can then be recycled to form new stars. We note that the parameter f_{st} is different to the parameter f_{trans} defined in Thomas et al. (1999). The latter is not an accumulated value and cannot be larger than one. ^(b) Models with $t_{\text{sf}} < 25$ Myr and $SFR > 10^4 M_{\odot}/\text{yr}$ are also computed in order to cover the lower right corner of likelihood map in Fig. 3, 5, and 7 below.

that of $[Z/X]$. It is known now that the iron abundance is not a good proxy for the total metallicity of an elliptical galaxy since the $[\text{Fe}/\text{H}]$ varies very little with the galaxy mass compared to metallicity that increases significantly with galaxy mass (e.g. Johansson et al. 2012, Conroy et al. 2014, and Kriek et al. 2019).

To check the consistency between our model and Thomas et al. (2005, their equation 5), we assume a fixed f_{st} value of 0.5² and fit only the $[\text{Mg}/\text{Fe}]$ observation, that is, instead of Eq. 3 we assume in this section:

$$p(M_{\text{dyn}}, f_{\text{st}} = 0.5, t_{\text{sf}}) = p_{\text{Mg/Fe}}. \quad (4)$$

The resulting likelihood map for galaxies with different combinations of masses and SFTs is shown in Fig. 3. The yellow (best-fit) region reproduces the Thomas et al. relation, shown as the dashed line. Considering that there are several differences between the two models (e.g., the parameter f_{st} might be different, we apply a Kroupa IMF as the gwIMF while Thomas et al. (2005) apply the Salpeter IMF as the gwIMF, the normalization and delay time distribution of SNIa are not identical, the computer codes are entirely different and independently developed, etc.), the degree of agreement is impressive.

Therefore, the galaxy chemical evolution model published in Yan et al. (2019) is consistent with other existing models.

4.2. Fitting also the metallicity

4.2.1. Solutions with fixed star formation fraction

Having tested that our model is in line with the previous study, we take the observational $[Z/X]$ values into consideration. As can be expected, a model with f_{st} being fixed cannot reproduce the increasing $[Z/X]$ for more massive galaxies as is shown in Fig. 4 (the computations for this figure all assume $f_{\text{st}} = 0.5$). A variable f_{st} is necessary.

4.2.2. Solutions with a variable star formation fraction

Galaxies with a higher mass require a higher f_{st} value as they are more metal-rich. The most likely f_{st} (resulting in the highest p as defined by Eq. 3 above) for each M_{dyn} is applied. The likelihood map and the corresponding f_{st} value for each galaxy mass are shown in Figs. 5 and Fig. 6, respectively.

The result suggests that the SFT for massive galaxies has an even smaller value than that deduced by Thomas et al. (2005) (shown as the dashed line). This is because massive galaxies have a higher averaged stellar metallicity while the metal-rich stars have a lower $[\text{Mg}/\text{Fe}]$ yield. As the increasing $[Z/X]$ ratio is now reproduced by an increasing f_{st} , the galactic $[\text{Mg}/\text{Fe}]$

² Fixed f_{st} values of 0.3, 0.4, 0.6, and 0.7 were also tested while the best fit value is 0.5.

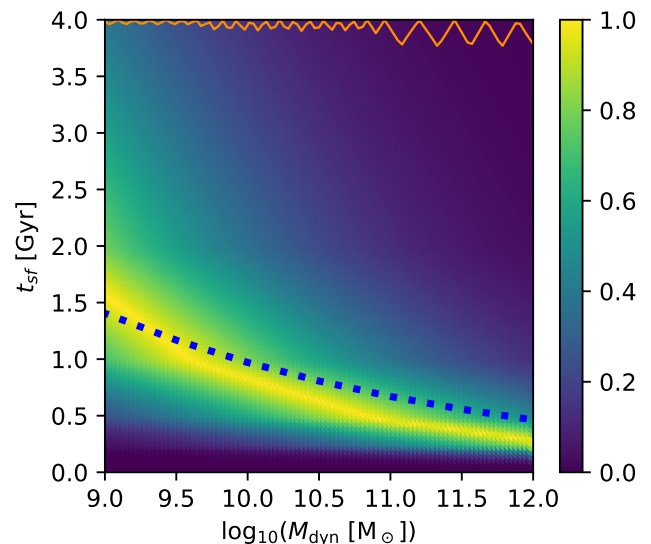


Fig. 3. Likelihood (shown as the colour map) for a given SFT, t_{sf} , and galaxy dynamical mass, M_{dyn} , as defined in Eq. 4 assuming an invariant canonical gwIMF and fitting only the $[\text{Mg}/\text{Fe}]$ observations. The blue dotted curve indicates the downsizing relation of Thomas et al. (2005). The thin orange curve is the value of the highest likelihood for any given M_{dyn} that follows the yellow ridge-line, sharing the y-axis with the likelihood colour-bar.

yield in the massive galaxies becomes lower and requires an even shorter SFT than before to fit with the high $[\text{Mg}/\text{Fe}]$ value of massive ellipticals. This is demonstrated by the green and blue filled circles in Figs. 1 and 2.

The even shorter SFT is unrealistic in hydrodynamical simulations with a non-zero gas-recycling time (see Section 1). It also contradicts the lower SFT limit of about 0.4 Gyr set by the observation of the $[\text{C}/\text{Mg}]$ values as argued in Johansson et al. (2012). Thus, no solution can be found with our fiducial setup outlined in Section 3.1. In the following section, we drop some of the assumptions in order to find a solution.

5. Possible modifications of the fiducial model

Here we explore whether the above result is robust under different assumptions on the stellar yield table and the IMF.

Since the first report of the $[\text{Mg}/\text{Fe}]$ –galaxy-mass relation (Worthey et al. 1992), two alternative explanations have been proposed: a selective galactic wind, or a change of the gwIMF. The selective galactic wind is difficult to study theoretically. It is also disfavoured by Matteucci (1994) because most stellar populations would have already formed before the onset of strong

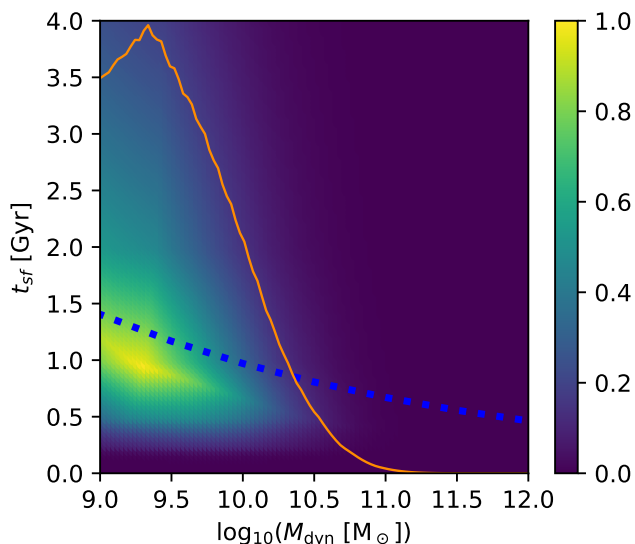


Fig. 4. Same as Fig. 3 but now fitting the [Mg/Fe] and [Z/X] observations simultaneously with the likelihood calculated by Eq. 3 and assuming a fixed f_{st} value of 0.5. No solution can be found for massive galaxies since they are more metal-rich, requiring a higher f_{st} value (see Fig. 5 and 6 below).

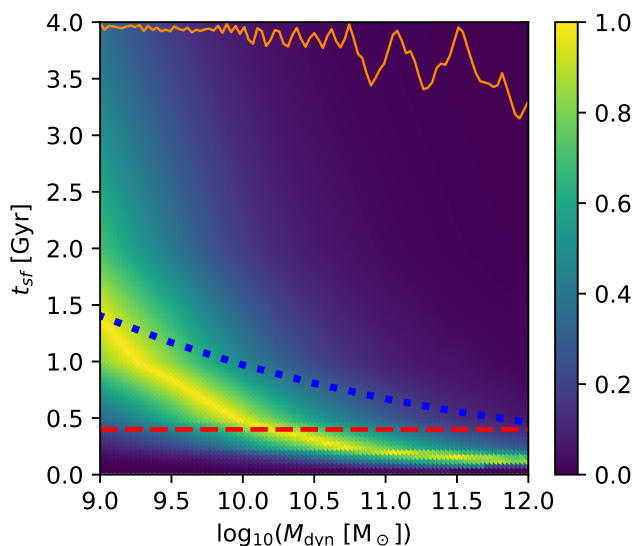


Fig. 5. Same as Fig. 4 but with different f_{st} values for each galaxy mass. The f_{st} is shown in Fig. 6 below. It is now possible to find solutions for high- and low-mass galaxies but the required SFT for the massive galaxies are excessively short compared to the 0.4 Gyr limit given by Johansson et al. (2012) shown as the red dashed line (see text).

galactic wind. Nevertheless, the idea can be explored with ad-hoc assumptions (e.g. Yates et al. 2013). On the other hand, a modification of the gwIMF has been expected and discussed for a long time (Thomas et al. 1999; Nagashima et al. 2005; Recchi et al. 2009; Spolaor et al. 2010; Gargiulo et al. 2015; Martín-Navarro 2016; Fontanot et al. 2017; Martín-Navarro et al. 2018; Barber et al. 2018), which, as we argue below, is the most promising solution.

Other possible modifications of the model such as more sophisticated SFHs, alternative delay time distributions (DTDs) of

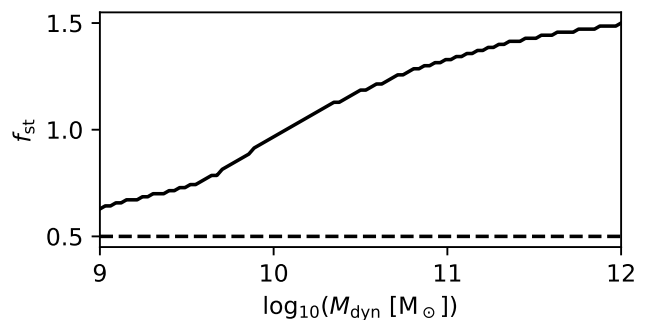


Fig. 6. Constant $f_{\text{st}} = 0.5$ assumed for the calculations shown in Figs. 3 and 4 (dashed line) and the corresponding accumulated star formation fraction, f_{st} , for the best-fit solutions for each dynamical mass, M_{dyn} , shown in Fig. 5 (solid curve). As explained in Table. 1, f_{st} can be higher than one.

SNIa events, and stellar rotation speed considerations are beyond the scope of the current study and we do not discuss these for now.

5.1. Modifying the stellar yield table

The stellar total yield of element i in our model is assumed to be a function of the stellar initial mass and its metallicity, $y_i(Z_*, M_*)$. For example, the element yield of a star with given mass and metallicity can be expressed as

$$y_{ijk}(M_* = M_j, Z_* = Z_k) = a_i + b_{ij} \cdot M_j + c_{ik} \cdot Z_k + O(M_j, Z_k), \quad (5)$$

where O represents the higher-order terms.

Sections 5.1.1 and 5.1.2 discuss the cases of modifying parameters b_{ij} and c_{ik} , respectively.

5.1.1. As a function of stellar initial mass, M_*

If the element-yields–stellar-mass relation is modified (e.g. parameter b_{ij} in Eq. 5), the stellar-population-averaged yield can be different, but the change would be the same for all galaxies since they have the same gwIMF. The modification can then be accounted for by a single adjustment of the stellar-population averaged yield, which alters all the [Mg/Fe] results (e.g. thin coloured lines in Fig. 2) and/or all the [Z/X] results (e.g. thin coloured lines in Fig. 1) by the same amount. The modifications of the [Mg/Fe] and [Z/X] results could be similar when the Mg yield is modified since it is linked with the oxygen yield which is the most abundant metal element. As we verified, ignoring the [Z/X] modification does not change our conclusions because [Z/X] affects mostly the determination of the f_{st} parameter rather than t_{sf} .

As mentioned in Section 4.2.2, SFT should be at least 0.4 Gyr for all galaxies. To increase the required SFT values, a higher galactic IMF-weighted [Mg/Fe] yield is needed. The theoretical stellar Mg yields can indeed be higher than the current applied values (Portinari et al. 1998, their section 9.7) by as much as 0.3 dex (Thomas et al. 1998; Karlsson & Gustafsson 2005; Philcox et al. 2018). Assuming that the stellar yield difference has a linear effect on the galactic yield, the gwIMF-weighted [Mg/Fe] yield might be higher also by about 0.3 dex.

With a higher [Mg/Fe] yield, the best-fitting SFTs of massive ellipticals can reach 0.4 Gyr. However, the best-fitting SFT for the low-mass galaxies increases more dramatically. This is

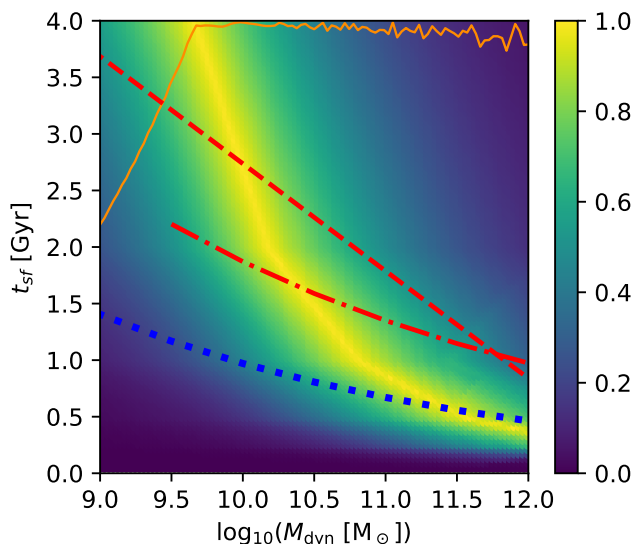


Fig. 7. Same as Fig. 5 but assuming a higher galactic Mg yield by 0.15 dex (40%) increase. The additional red dashed line and the red dash-dot line are the half-mass formation timescale determined with the stellar population synthesis method, independent of our chemical evolution constraints, given by de La Rosa et al. (2011) and McDermid et al. (2015), respectively. We note that the red lines are rough estimations (see Section 6 below) and may shift horizontally by 1 or 2 dex depending on the amount of gas and dark matter involved in the estimation of M_{dyn} (see Section 2.3), which would not affect our conclusions.

shown in Fig. 7 with a model assuming a galactic [Mg/Fe] yield higher by 0.15 dex than the fiducial model (while the [Z/X] galactic yield is not modified). The best-fitting SFTs for low-mass galaxies become much longer than other independent observational estimations (see Fig. 7 and Section 6 below), suggesting that the required SFT to reproduce the [Mg/Fe] observations in such a model is not fulfilled by real galaxies.

In summary, we find no solution which satisfies the SFT constraints of massive and low-mass galaxies simultaneously solely by modifying the stellar yield table as a function of the stellar initial mass. It might be possible to find a solution by combining the stellar yield modification with a specific galactic-wind-strength–galaxy-mass relation, but there will be parameters to be fine-tuned while other explanations could be simpler.

5.1.2. As a function of stellar initial metallicity

If the metal-rich stars produce more magnesium than the currently applied value, it is in principle possible to increase the required SFT of massive galaxies that have a higher metallicity while not affecting the low-mass galaxies. It has been suggested that metallicity may correlate with the rotation speed of the stars which leads to a different yield, which seems to be in line with this scenario. The consideration of yields modified by stellar rotation speed is very uncertain, but Romano et al. (2019) demonstrated a useful approach to this possibility.

We note that although the average stellar [Mg/Fe] and [Z/X] of galaxies in different mass bins agrees with the above ansatz, the individual low-mass galaxies, which have vastly different [Z/X] but similar [Mg/Fe], do not agree and require another explanation. This possibly involves galactic inflow and selective galactic winds. However, our current work considers the simple situation without gas flow (see Yan et al. 2019).

In any case, we disfavour such a solution where the stellar yield is modified as a function of galaxy mass since it mimics the effect of a variable gwIMF (see the following section). These two scenarios are degenerate.

In conclusion, merely applying a different stellar yield cannot explain the [Mg/Fe] and [Z/X] observations. The estimation of SFT when considering both observations leads to a more severe downsizing relation (such as Fig. 5 or Fig. 7) which is not reconcilable with either hydrodynamical simulations of the formation of early-type galaxies or with independent estimations (red lines in the aforementioned figures, described in Sections 4.2.2 and 6 below).

5.2. Modifying the gwIMF

5.2.1. Universal invariant non-canonical gwIMF

If the gwIMF is universal but different from (within the observational uncertainty) the assumed one, our conclusion may be compromised.

For a steeper gwIMF which forms fewer massive stars per low-mass star, Thomas et al. (1999) shows that the top-light gwIMF leads to lower α element production and requires a shorter SFT of about 10^8 yr to fulfil a [Mg/Fe] value of 0.2 dex for massive ellipticals. Martín-Navarro (2016) again, motivated by the recent evidence supporting a bottom-heavy gwIMF for massive ellipticals, shows that a steep gwIMF requires an extreme and unrealistically short SFT.

For a flatter gwIMF, Arrigoni et al. (2010) claimed that they can reproduce both [Mg/Fe] and [Z/X] observations with an invariant and slightly top-heavy gwIMF. However, their calculation adopted a wrong stellar iron yield as pointed out in the erratum declaration in Arrigoni et al. (2012). This mistake leads to a higher [Mg/Fe] yield for stars with a higher initial metallicity, which reverses the real relation (see Section 1) and allows (erroneously) explanation of the correlation between [Mg/Fe] and [Z/X]. With the correct stellar yield adopted, Thomas et al. (1999) claim that a top-heavy gwIMF has no significant effect on the simulated [Mg/Fe] value.

We note that the gwIMF of massive ellipticals is probably bottom-heavy and top-heavy at the same time (Jeřábková et al. 2018; Yan et al. 2019) and it could have a more complicated shape. It is beyond the scope of this work to exclude a comprehensive set of possible shapes of an invariant gwIMF by simulating all the difference cases. In general however, a universal invariant gwIMF, no matter what its formulation, applies to all galaxies. Therefore, the model would encounter the same difficulty as in Section 5.1.1, meaning that there is no solution for both high- and low-mass galaxies.

5.2.2. Variable gwIMF

As is shown above, it is difficult to find a solution under the standard assumptions. The fact that metal-poor stars in the Milky Way have a large scatter of [Mg/Fe] values (e.g. observations compiled in Prantzos et al. 2018) and the high [Mg/Fe] value of the ultra-diffuse galaxy DGSAT I that is supposed to have an extended (≈ 3 Gyr) SFH (Martín-Navarro et al. 2019) support a non-universal gwIMF. Indeed, observational evidence is now pointing towards the IMF being dependent on the metallicity and density of molecular cloud cores on parsec scales (Marks et al. 2012) and varying systematically predominantly with the SFR on galaxy scales (for recent reviews, see Kroupa et al. 2013 and Hopkins 2018).

With a top-heavy gwIMF for massive galaxies, as suggested by the IGMF theory (Kroupa et al. 2013; Yan et al. 2017; Jeřábková et al. 2018), it is possible to fit [Mg/Fe] and [Z/X] with a milder downsized SFT relation (Recchi et al. 2009). Not only [Mg/Fe], but also other element abundance ratios of high-redshift starburst galaxies appear to be better understood with a top-heavy gwIMF (Palla et al. 2019). The scenario that more massive galaxies have a more top-heavy gwIMF also explains other observational properties that are difficult to understand under the invariant gwIMF scheme. For example, the early enrichment of the massive ellipticals, the systematical variation of galaxy photometric features (Hoversten & Glazebrook 2008; Meurer et al. 2009; Lee et al. 2009; Gunawardhana et al. 2011), the high metal-to-star-mass ratio of massive galaxy clusters (Renzini & Andreon 2014; Urban et al. 2017), and the systematic variation of galactic isotope abundances (Romano et al. 2017; Zhang et al. 2018) readily follow if the gwIMF varies systematically as encompassed by the IGMF theory.

Therefore, some formalism of a systematically varying gwIMF (e.g. the IGMF theory) appears to be the most probable solution so far to explain the [Mg/Fe] and metallicity of elliptical galaxies. More importantly, when compared with other possible solutions (e.g. a fine-tuned and coordinated SFH for all galaxies; a different SNIa DTD; and stellar yield variation as a function of stellar rotation speed) the gwIMF variation provides predictions that are easier to test and to falsify. In a companion paper (Yan et al. 2020, in prep.), we address the galaxy-mass–SFT relation given the [Mg/Fe] and [Z/X] constraints using the IGMF theory as an alternative to the invariant canonical gwIMF applied here.

6. Comparison with independent SFT constrains

The SFT applied in galaxy evolution models must satisfy direct observational constraints even though the current constraints are neither accurate nor reliable (Renzini 2006).

Schiavon (2007); de La Rosa et al. (2011); McDermid et al. (2015) performed stellar population synthesis of local early-type galaxies based on galactic line-strength indices or full spectral fitting, supporting the downsizing of t_{st} with the most massive galaxies formed on a billion-year timescale with SFTs being longer for low-mass galaxies. On the other hand, Carnall et al. (2018), who recovered the SFHs of a large ensemble of galaxies using photometric data, suggests that the SFT of local quiescent galaxies with a stellar-mass above $10^{10} M_{\odot}$ does not correlate with stellar mass.

We note that these synthesis studies are based on an invariant gwIMF while a non-universal gwIMF would significantly change the results (Ferré-Mateu et al. 2013).

Also, there are some important drawbacks of this kind of method. Firstly, there is no guarantee that the SPS solution is unique. The SFH solution based on the integrated galactic light of all stellar populations always suffers from degeneracy and a prior assumption on the shape (and the smoothness) of the SFH, which may or may not be realistic, always needs to be made. Since the spectral features are dominated by the stellar population that is most luminous, the SPS method has a larger uncertainty for the modelled older stellar populations, and is therefore less reliable for galaxies with a longer SFT. Secondly, the best-fitting solution may not be realistic. Artificial simple stellar populations (SSPs) with different ages and metallicities are synthesized to fit the spectrum of the observed galaxy but there is no guarantee that these populations can be self-consistently generated under the additional constraint of needing to also satisfy the metal enrichment history of the galaxy. Finally, the abundance

ratios (notably the α -enhancement) are either not being considered, that is, the stellar population model is only a function of its age and metallicity, or when considered they have the same issue regarding the chemical evolution self-consistency.

Therefore, the present SPS studies are affected by random and substantial systematic errors. Nevertheless, we consider these results from different groups as an envelope of solutions accounting for systematic errors. Significant SFT deviations from these results are unlikely. The suggested SFTs from population synthesis studies are plotted in Fig. 7 as red lines. It appears that they do not agree with the suggested SFT from chemical evolution simultaneously fitting both [Mg/Fe] and [Z/X] data as mentioned above in Section 5.1.1 (cf. chemo-archaeological downsizing, Fontanot et al. 2009). The chemo-archaeological study yields either SFTs of massive galaxies that are too short as shown in Fig. 5 or SFTs of low-mass galaxies that are too long as shown in Fig. 7.

Another independent approach estimating the SFT of galaxies is to count the galaxies and map the evolution with redshift of the comoving number density of quiescent elliptical galaxies (Bell et al. 2004). Due to the limited ability of high-redshift observations and thus selection bias as well as the possibility that a pseudo-evolution may be deduced if an incorrect cosmological model is applied (Balakrishna Subramani et al. 2019), the constraints on SFT are weak. Besides, if the gwIMF at higher redshift were different, the estimation of the galaxy mass and SFR would be systematically biased (Jeřábková et al. 2018, their figure 7). The consensus assuming the invariant canonical gwIMF is that most massive elliptical galaxies should have formed above redshift 3, which limits the SFT to less than 2 Gyr considering the age of the Universe in consensus cosmology. Low-mass ellipticals do not have such limitations. To constrain the SFT instead of the ending time, one might try to count the galaxies as a function of redshift when they are still forming stars. For example, Reddy et al. (2006) show that the distant red galaxies, which are likely to be dusty starburst precursors to elliptical galaxies, appear to be distributed evenly from redshift 1 to over 3.5. It is not trivial to interpret such observations however because the SFHs of the snapshot high-redshift galaxies are not known and they cannot be easily linked to a low-redshift counterpart. Possible galaxy mergers require additional assumptions to perform such studies. We note, however, that over the past 6 Gyr the number fraction of elliptical galaxies among all galaxies with a baryonic mass larger than $10^{10} M_{\odot}$ remained unchanged at about 3.5% (Delgado-Serrano et al. 2010), suggesting that mergers may not be an important concern.

In summary, the available evidence supports the idea that massive ellipticals start and finish their star formation at early times. A mildly downsizing and a no-downsizing SFT–galaxy-mass relation (Yan et al. 2020, in prep.) are both consistent with current observational constraints. On the other hand, severe downsizing, as required in the invariant gwIMF scheme, is not allowed, given the data.

7. Conclusion

In this work, a grid of chemical evolution models is computed for elliptical galaxies with different gas-to-star transformation ratios (f_{st}) and different SFHs (Section 3.1). The results are compared with observations (Section 3.2).

First, we compare only the [Mg/Fe]–galaxy-mass relation, in which case the downsizing of SFT suggested by Thomas et al. (2005) is reproduced (Section 4.1). This validates our chemical evolution code (Yan et al. 2019).

Furthermore, we fitted both the $[Z/X]$ and $[Mg/Fe]$ observations simultaneously (Section 4.2). The results suggest a more severe downsizing relation due to the lower $[Mg/Fe]$ yield of massive metal-rich stars.

The uncertainty of our method and possible modifications of the applied assumptions are discussed and we conclude that, under the invariant gwIMF paradigm, a severe downsizing relation is always required no matter what stellar yield modification is applied (Section 5.1 and 5.2.1).

Finally, we show that the severe downsizing relation is either not consistent with the SFT estimation from stellar population synthesis methods (Section 6) and/or it is not consistent with $[C/Mg]$ observations and it is difficult to reconcile with hydrodynamical simulations.

Among the remaining possible solutions, we find that a systematically varying gwIMF is the most promising and well-supported (Section 5.2.2). This is detailed in the accompanying paper (Yan et al. 2020, in prep.).

In summary:

- We tested that our newly developed chemical evolution code GalIMF (Yan et al. 2019) is consistent with previous studies.
- We conclude that $[Mg/Fe]$ as an indicator of the SFT is incorrect if $[Z/X]$ is not taken into consideration.
- Furthermore, we suggest that an invariant gwIMF is unable to reproduce both $[Mg/Fe]$ –galaxy-mass and $[Z/X]$ –galaxy-mass observations unless an extreme downsizing relation (the yellow ridge-line in Fig. 5) is accepted.

Acknowledgements. ZY acknowledges financial support from the China Scholarship Council (CSC, file number 201708080069). TJ acknowledges support by the Erasmus+ programme of the European Union under grant number 2017-1-CZ01- KA203-035562. The development of our chemical evolution model applied in this work benefited from the International Space Science Institute (ISSI/ISSI-BJ) in Bern and Beijing, thanks to the funding of the team “Chemical abundances in the ISM: the litmus test of stellar IMF variations in galaxies across cosmic time” (Donatella Romano and Zhi-Yu Zhang). Last but not least, we acknowledge correction and fruitful comments from Daniel Thomas.

References

Anders, E. & Grevesse, N. 1989, *Geochim. Cosmochim. Acta*, 53, 197
 Arrigoni, M., Trager, S. C., Somerville, R. S., & Gibson, B. K. 2010, *MNRAS*, 402, 173
 Arrigoni, M., Trager, S. C., Somerville, R. S., & Gibson, B. K. 2012, *Monthly Notices of the Royal Astronomical Society*, 424, 800
 Balakrishna Subramani, V., Kroupa, P., Shenavar, H., & Muralidhara, V. 2019, *MNRAS*, 488, 3876
 Barber, C., Crain, R. A., & Schaye, J. 2018, *MNRAS*, 479, 5448
 Bell, E. F., Wolf, C., Meisenheimer, K., et al. 2004, *ApJ*, 608, 752
 Binney, J. & Tremaine, S. 2008, *Galactic Dynamics: Second Edition*
 Buote, D. A. & Barth, A. J. 2019, *ApJ*, 877, 91
 Burstein, D., Bender, R., Faber, S., & Nolthenius, R. 1997, *AJ*, 114, 1365
 Calura, F. & Menci, N. 2009, *Monthly Notices of the Royal Astronomical Society*, 400, 1347
 Calura, F. & Menci, N. 2011, *Monthly Notices of the Royal Astronomical Society*, 413, L1
 Carnall, A. C., McLure, R. J., Dunlop, J. S., & Davé, R. 2018, *MNRAS*, 480, 4379
 Chieffi, A. & Limongi, M. 2004, *ApJ*, 608, 405
 Conroy, C., Graves, G. J., & van Dokkum, P. G. 2014, *ApJ*, 780, 33
 Cowie, L. L., Songaila, A., Hu, E. M., & Cohen, J. G. 1996, *AJ*, 112, 839
 Dabringhausen, J. 2019, *MNRAS*, 490, 848
 de La Rosa, I. G., La Barbera, F., Ferreras, I., & de Carvalho, R. R. 2011, *MNRAS*, 418, L74
 De Lucia, G., Fontanot, F., & Hirschmann, M. 2017, *MNRAS*, 466, L88
 De Masi, C., Matteucci, F., & Vincenzo, F. 2018, *MNRAS*, 474, 5259
 Delgado-Serrano, R., Hammer, F., Yang, Y. B., et al. 2010, *A&A*, 509, A78
 Faber, S. M. & Jackson, R. E. 1976, *ApJ*, 204, 668
 Ferré-Mateu, A., Vazdekis, A., & de la Rosa, I. G. 2013, *MNRAS*, 431, 440
 Fontanot, F. 2014, *MNRAS*, 442, 3138

Fontanot, F., De Lucia, G., Hirschmann, M., et al. 2017, *MNRAS*, 464, 3812
 Fontanot, F., De Lucia, G., Monaco, P., Somerville, R. S., & Santini, P. 2009, *MNRAS*, 397, 1776
 Gallazzi, A., Charlot, S., Brinchmann, J., White, S. D. M., & Tremonti, C. A. 2005, *MNRAS*, 362, 41
 Gargiulo, I. D., Cora, S. A., Padilla, N. D., et al. 2015, *MNRAS*, 446, 3820
 Gibson, B. K., Loewenstein, M., & Mushotzky, R. F. 1997, *MNRAS*, 290, 623
 Johawardhana, M. L. P., Hopkins, A. M., Sharp, R. G., et al. 2011, *MNRAS*, 415, 1647
 Hopkins, A. M. 2018, *PASA*, 35 [arXiv:1807.09949]
 Hoversten, E. A. & Glazebrook, K. 2008, *ApJ*, 675, 163
 Jeřábková, T., Hasani Zonoozi, A., Kroupa, P., et al. 2018, *A&A*, 620, A39
 Johansson, J., Thomas, D., & Maraston, C. 2012, *MNRAS*, 421, 1908
 Karlsson, T. & Gustafsson, B. 2005, *A&A*, 436, 879
 Kormendy, J. 1977, *ApJ*, 218, 333
 Kriek, M., Price, S. H., Conroy, C., et al. 2019, *ApJ*, 880, L31
 Kroupa, P. 2001, *MNRAS*, 322, 231
 Kroupa, P., Weidner, C., Pflamm-Altenburg, J., et al. 2013, *The Stellar and Sub-Stellar Initial Mass Function of Simple and Composite Populations* (Springer Science+Business Media Dordrecht), 115
 Lee, J. C., Gil de Paz, A., Tremonti, C., et al. 2009, *ApJ*, 706, 599
 Liu, Y., Ho, L. C., & Peng, E. 2016a, *ApJ*, 829, L26
 Liu, Y., Peng, E. W., Blakeslee, J., et al. 2016b, *ApJ*, 818, 179
 Maoz, D. & Mannucci, F. 2012, *PASA*, 29, 447
 Marigo, P. 2001, *A&A*, 370, 194
 Marks, M., Kroupa, P., Dabringhausen, J., & Pawłowski, M. S. 2012, *MNRAS*, 422, 2246
 Martín-Navarro, I. 2016, *MNRAS*, 456, L104
 Martín-Navarro, I., Romanowsky, A. J., Brodie, J. P., et al. 2019, *MNRAS*, 484, 3425
 Martín-Navarro, I., Vazdekis, A., Falcón-Barroso, J., et al. 2018, *MNRAS*, 475, 3700
 Matteucci, F. 1994, *A&A*, 288, 57
 Matteucci, F. 2012, *Chemical Evolution of Galaxies* (Springer-Verlag Berlin Heidelberg)
 McDermid, R. M., Alatalo, K., Blitz, L., et al. 2015, *MNRAS*, 448, 3484
 Meurer, G. R., Wong, O. I., Kim, J. H., et al. 2009, *ApJ*, 695, 765
 Nagashima, M., Lacey, C. G., Okamoto, T., et al. 2005, *Monthly Notices of the Royal Astronomical Society*, 363, L31
 Nomoto, K., Kobayashi, C., & Tominaga, N. 2013, *ARA&A*, 51, 457
 Okamoto, T., Nagashima, M., Lacey, C. G., & Frenk, C. S. 2017, *MNRAS*, 464, 4866
 Palla, M., Calura, F., Fan, X., et al. 2019, arXiv e-prints, arXiv:1908.06832
 Pantoni, L., Lapi, A., Massardi, M., Goswami, S., & Danese, L. 2019, *ApJ*, 880, 129
 Philcox, O., Rybizki, J., & Gutcke, T. A. 2018, *ApJ*, 861, 40
 Pipino, A., Devriendt, J. E. G., Thomas, D., Silk, J., & Kaviraj, S. 2009, *A&A*, 505, 1075
 Pipino, A. & Matteucci, F. 2004, *MNRAS*, 347, 968
 Pipino, A. & Matteucci, F. 2006, in *American Institute of Physics Conference Series*, Vol. 847, *Origin of Matter and Evolution of Galaxies*, ed. S. Kubono, W. Aoki, T. Kajino, T. Motobayashi, & K. Nomoto, 461–463
 Portinari, L., Chiosi, C., & Bressan, A. 1998, *A&A*, 334, 505
 Prantzos, N., Abia, C., Limongi, M., Chieffi, A., & Cristallo, S. 2018, *MNRAS*, 476, 3432
 Recchi, S., Calura, F., & Kroupa, P. 2009, *A&A*, 499, 711
 Recchi, S. & Kroupa, P. 2015, *MNRAS*, 446, 4168
 Reddy, N. A., Steidel, C. C., Fadda, D., et al. 2006, *ApJ*, 644, 792
 Renzini, A. 2006, *ARA&A*, 44, 141
 Renzini, A. & Andreon, S. 2014, *MNRAS*, 444, 3581
 Romano, D., Matteucci, F., Zhang, Z.-Y., Ivison, R. J., & Ventura, P. 2019, arXiv e-prints, arXiv:1907.09476
 Romano, D., Matteucci, F., Zhang, Z.-Y., Papadopoulos, P. P., & Ivison, R. J. 2017, *MNRAS*, 470, 401
 Schiavon, R. P. 2007, *ApJS*, 171, 146
 Segers, M. C., Schaye, J., Bower, R. G., et al. 2016, *MNRAS*, 461, L102
 Spolaor, M., Kobayashi, C., Forbes, D. A., Couch, W. J., & Hau, G. K. T. 2010, *MNRAS*, 408, 272
 Thomas, D., Greggio, L., & Bender, R. 1998, *MNRAS*, 296, 119
 Thomas, D., Greggio, L., & Bender, R. 1999, *MNRAS*, 302, 537
 Thomas, D., Maraston, C., Bender, R., & Mendes de Oliveira, C. 2005, *ApJ*, 621, 673
 Thomas, D., Maraston, C., Schawinski, K., Sarzi, M., & Silk, J. 2010, *MNRAS*, 404, 1775
 Thomas, J., Saglia, R. P., Bender, R., et al. 2011, *MNRAS*, 415, 545
 Trager, S. C., Faber, S. M., Worthey, G., & González, J. J. 2000, *AJ*, 120, 165
 Urban, O., Werner, N., Allen, S. W., Simionescu, A., & Mantz, A. 2017, *MNRAS*, 470, 4583
 Vazdekis, A., Casuso, E., Peletier, R. F., & Beckman, J. E. 1996, *ApJS*, 106, 307
 Vazdekis, A., Peletier, R. F., Beckman, J. E., & Casuso, E. 1997, *ApJS*, 111, 203
 Vincenzo, F., Matteucci, F., Recchi, S., et al. 2015, *MNRAS*, 449, 1327
 Weidner, C., Ferreras, I., Vazdekis, A., & La Barbera, F. 2013, *MNRAS*, 435, 2274
 Worthey, G., Faber, S. M., & Gonzalez, J. J. 1992, *ApJ*, 398, 69
 Yan, Z., Jerabkova, T., & Kroupa, P. 2017, *A&A*, 607, A126
 Yan, Z., Jerabkova, T., & Kroupa, P. 2020, *A&A*, in prep.
 Yan, Z., Jerabkova, T., Kroupa, P., & Vazdekis, A. 2019, *A&A*, 629, A93
 Yates, R. M., Henriques, B., Thomas, P. A., et al. 2013, *MNRAS*, 435, 3500
 Zhang, Z.-Y., Romano, D., Ivison, R. J., Papadopoulos, P. P., & Matteucci, F. 2018, *Nature*, 558, 260